JOURNAL
OF THE
AMERICAN
CHEMICAL
SOCIETY

Experimental and Theoretical Studies on the Thermal Decomposition of Heterocyclic Nitrosimines[1]

Richard A. Bartsch,* Yeh Moon Chae, Sihyun Ham, and David M. Birney*

Contribution from the Department of Chemistry and Biochemistry, Texas Tech University, Lubbock, Texas 79409-1061

Received March 12, 2001

Abstract: A series of substituted 2-nitrosiminobenzothiazolines (**2**) were synthesized by the nitrosation of the corresponding 2-iminobenzothiazolines (**6**). Thermal decomposition of **2a**−**f** and of the seleno analogue **7** in methanol and of 3-methyl-2-nitrosobenzothiazoline (**2a**) in acetonitrile, 1,4-dioxane, and cyclohexane followed first-order kinetics. The activation parameters for thermal deazetization of **2a** were measured in cyclohexane ($\Delta H^{\ddagger} = 25.3 \pm 0.5$ kcal/mol, $\Delta S^{\ddagger} = 1.3 \pm 1.5$ eu) and in methanol ($\Delta H^{\ddagger} = 22.5 \pm 0.7$ kcal/mol, $\Delta S^{\ddagger} = -12.9 \pm 2.1$ eu). These results indicate a unimolecular decomposition and are consistent with a proposed stepwise mechanism involving cyclization of the nitrosimine followed by loss of N_2. The ground-state conformations of the parent nitrosiminothiazoline (**9a**) and transition states for rotation around the exocyclic C=N bond, electrocyclic ring closure, and loss of N_2 were calculated using ab initio molecular orbital theory at the MP2/6-31G* level. The calculated gas-phase barrier height for the loss of N_2 from **9a** (25.2 kcal/mol, MP4(SDQ, FC)/6-31G*//MP2/6-31G* + ZPE) compares favorably with the experimental barrier for **2a** of 25.3 kcal/mol in cyclohexane. The potential energy surface is unusual; the rotational transition state **9a-rot-ts** connects directly to the orthogonal transition state for ring-closure **9aTS**. The decoupling of rotational and pseudopericyclic bond-forming transition states is contrasted with the single pericyclic transition state (**15TS**) for the electrocyclic ring-opening of oxetene (**15**) to acrolein (**16**). For comparison, the calculated homolytic strength of the N−NO bond is 40.0 kcal/mol (MP4(SDQ, FC)/6-31G*//MP2/6-31G* + ZPE).

Introduction

The chemistry of nitroso compounds has been a subject of great interest to a broad audience. The most well-known reactions are ones that generate and trap nitric oxide (NO).[2] These reactions have recently been shown to be important in a variety of biochemical signaling pathways,[3] and some of these pathways have captured the attention of nonchemists as well.[4] NO is also believed to be involved in the nitrogen cycle.[5] Historically, nitrosimines were studied because they were potential carcinogens.[6] More recently *N*-nitrosoureas have been

explored as anticancer and antithrombotic drugs.[7] The most widely studied reactions of nitroso compounds have been the homolysis to form NO.[2b] However, other reactions are known; for example, *N*-nitrosoaziridenes lose N_2O to form alkenes in a

(1) Taken in part from the MS thesis of Chae, Y. M. *Mechanism of the Thermal Decomposition of Heterocyclic Nitrosimines*; Washington State University, 1972; p 48.

(2) (a) Reszka, K. J.; Bilski, P.; Chignell, C. F. *J. Am. Chem. Soc.* **1996**, *118*, 8719−8720. (b) Cheng, J.-P.; Xian, M.; Wang, K.; Zhu, X.; Yin, Z.; Wang, P. G. *J. Am. Chem. Soc.* **1998**, *120*, 10266−10267. (c) Richter-Addo, G. B. *Acc. Chem. Res.* **1999**, *32*, 529−536. (d) Williams, D. L. H. *Acc. Chem. Res.* **1999**, *32*, 869−876. (e) Turjanski, A. G.; Leonik, F.; Estrin, D. A.; Rosenstein, R. E.; Doctorovich, F. *J. Am. Chem. Soc.* **2000**, *122*, 10468−10469. (f) Xian, M.; Xhu, X.-Q.; Lu, J.; Wen, Z.; Cheng, J.-P. *Org. Lett.* **2000**, *2*, 265−268. (g) Lü, J.-M.; Wittbrodt, J. M.; Wang, K.; Wen, Z.; Schlegel, H. B.; Wang, P. G.; Cheng, J.-P. *J. Am. Chem. Soc.* **2001**, *123*, 2903−2904. (h) Zhu, X.-Q.; He, J.-Q.; Li, Q.; Xian, M.; Lu, J.; Cheng, J.-P. *J. Org. Chem.* **2000**, *65*.

cheletropic fragmentation.[8] In contrast, *N*-nitrosimines (**1**) spontaneously lose nitrogen rather than NO.[6b,9] This gives the corresponding ketone, as illustrated in eq 1. Loss of nitrogen has been shown to be quantitative.[9a] In one earlier study, nitrogen evolution was shown to proceed via first-order kinetics ($t_{1/2}$ = 4.75 h) for **1** with R_1 = 4-MePh and R_2 = 2-MePh.[9b] Steric bulk and conjugation stabilize nitrosimines. For example, **1** with R_1 = *t*-Bu and R_2 = 2-MePh is stable for weeks, but no dialkylnitrosimines are known.[9b] The 3-substituted 2-nitrosimi-nobenzothiazonines (e.g., **2a**) are among the more stable derivatives known and require heating, for example in refluxing methanol, for deazetization.[6b]


$$\qquad\qquad (1)$$
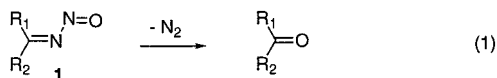
For the thermal reaction, a unimolecular, two-step mechanism has been proposed as shown in eq 2.[9b] In this mechanism, a concerted electrocyclization is envisioned to form the strained four-membered ring in **3**, followed by a presumably forbidden,[10] but highly exothermic, deazetization to give **4**. It was this unusual mechanism that first drew our attention to this reaction. The electrocyclic ring closure is, at first glance, a 4-electron process, analogous to the cyclization of butadiene[10] or acrolein.[10,11] This would be expected to involve rotation around the C=N bond coupled with C−O bond formation.[11] Interestingly, the calculated pathway reported herein finds those two motions to be uncoupled.

$$\qquad\qquad (2)$$

a R = Me   **c** R = Pr   **e** R = Bn
b R = Et   **d** R = Ph
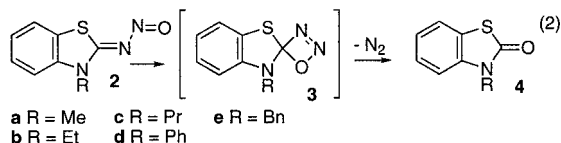
Photolysis of the strongly colored nitrosimines, such **2a**, gives rise to a variety of products that appear to have come from loss of NO and subsequent radical reactions (eq 3).[12] Similar products, indicative of radical reactions, are also observed in the thermolysis of sterically hindered nitrosimines (e.g., **1**, with R_1 = *t*-Bu and R_2 = 2-MePh).[13] Steric constraints were proposed disfavor the cyclic pathway (eq 2), thus diverting the reaction

to the radical pathway. The differences in the products observed in eq 2 as compared to eq 3 require that the two mechanisms be different and are consistent with a concerted reaction for the thermal deazetization of unhindered nitrosimines.

$$\qquad\qquad (3)$$
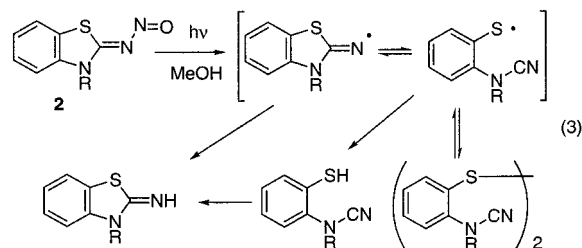
The work reported herein was undertaken to address several questions arising from the previous results and to explore the mechanism of the reaction. First, a detailed kinetic study was performed to obtain activation energies and to confirm that the formation of ketones is indeed first-order, in agreement with the observed first-order formation of nitrogen. Second, solvent effects were studied to give insight into the changes in charge distribution in going to the transition state. Last, ab initio calculations were used to explore the viability and the details of the proposed mechanism (eq 2). These predict that the reaction follows an unusual two-stage mechanism with two sequential transition states (C=N rotation followed by C−O bond formation) for the formation of the spiro intermediate (e.g., **3**).

Experimental Results and Discussion

A series of 3-substituted 2-nitrosiminobenzothiazolines (**2a−e**) as well as the disubstituted analogue **2f** were prepared following literature precedents, as shown in eq 4. The reaction of an arylamine hydrochloride with potassium thiocyanate gave the corresponding unsymmetrical thiourea **5**.[14] Oxidative cyclization with Br_2 gave the iminobenzothiazolines (**6**).[9a,14a,15] Finally, treatment with sodium nitrite in acetic acid gave the nitrosiminobenzothiazoline (**2**).[9a,b,15b] The nitrosiminobenzoselenazoline (**7**) was similarly prepared. However, an attempt to synthesize the oxygen analogue. **8**, gave only the corresponding ketone.

$$\qquad\qquad (4)$$
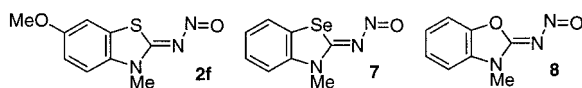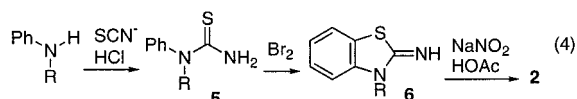
Thermal decomposition of 3-methyl-2-nitrosiminobenzothia-zoline (**2a**) has previously been shown to quantitatively evolve nitrogen.[9a] To confirm the identity and yield of the organic product as **4a**, **2a** was refluxed in methanol at 62.3° for 5.1 half-lives. A quantitative yield of 3-methyl-2-benzothiazolinone (**4a**) was estimated from the UV spectrum in methanol, based on independently synthesized **4a**. (See Supporting Information for details.)

(3) (a) Palmer, R. M. J.; Ferrige, A. G.; Moncada, S. *Nature* **1987**, *327*, 524. (b) Butler, A. R.; Williams, D. L. H. *Chem. Soc. Rev.* **1993**, *22*, 233−241.

(4) For the biochemical pathway involved in the biological activity of Viagra, see: (a) Terrett, N. K.; Bell, A. S.; Ellis, P. *Bioorg. Med. Chem. Lett.* **1996**, *6*, 1819. (b) Wilson, E. K. *Chem. Eng. News* **1998**, *76*, June 29, 29−33.

(5) Averill, B. A. *Chem. Rev.* **1996**, *96*, 2951−2964.

(6) (a) Anselme, J. P. *N−Nitrosamines*; American Chemical Society: Washington, DC, 1979. (b) Challis, B. C.; Challis, J. A. In *N-Nitrosoimines and N-Nitrosoimines*; Patai, S., Ed.; John Wiley and Sons: New York, 1982; Vol. 2, pp 1151−1223. (c) Olszewska, T.; Milewska, M. J.; Gdaniec, M.; Malusznska, H.; Polonski, T. *J. Org. Chem.* **2001**, *66*, 510−506.

(7) (a) Gnewuch, C. T.; Sosnovsky, G. *Chem. Rev.* **1997**, *97*, 829−1013. (b) Rehse, K.; Ciborski, T. *Arch. Pharm. (Weinheim, Ger.)* **1995**, *328*, 71.

(8) (a) Rundel, W.; Müller, E. *Chem. Ber.* **1963**, *96*, 2528−2531. (b) Clark, R. D.; Helmkamp, G. K. *J. Org. Chem.* **1964**, *29*, 1316−1320.

(9) (a) Besthorn, E. *Chem. Ber.* **1910**, *43*, 1519−1526. (b) Thoman, C. J.; Hunsberger, S. J.; Hunsberger, I. M. *J. Org. Chem.* **1968**, *33*, 2852−2857. (c) Akiba, K.-y.; Ishidawa, K.; Inamoto, K. *Bull. Chem. Soc. Jpn.* **1978**, *51*, 535−539.

(10) Woodward, R. B.; Hoffmann, R. *The Conservation of Orbital Symmetry*; Verlag Chemie, GmbH: Weinheim, 1970.

(11) Yu, H.; Chen, W.-T.; Goddard, J. D. *J. Am. Chem. Soc.* **1990**, *112*, 7529−7537.

(12) Akiba, K.; Fukawa, I.; Mashita, K.; Inamoto, N. *Tetrahedron Lett.* **1968**, 2859−2862.

(13) Jappy, J.; Preston, P. N. *Tetrahedron Lett.* **1970**, 1157−1160.

(14) (a) Passing, H. *J. Prakt. Chem.* **1939**, *153*, 1−25. (b) Fairful, A. E. S.; Peak, D. A. *J. Chem. Soc.* **1955**, 796−802.

(15) (a) Fuchs, K.; Grauaug, E. *Chem. Ber.* **1928**, *61*, 57−65. (b) Tsuda, K.; Fukushima, S. *J. Pharm. Soc., Jpn.* **1942**, *62*, 64.

Table 1. Rate of Decomposition of 3-Substituted 2-Nitrosiminobenzothiazolines **2a**−**f** and of **7** in Methanol at 62.3°

	3-substituent	6-substituent	$k_1 \times 10^5$ sec^{-1}	relative rate	σ^*
2a	CH$_3$	H	2.06^a	1.00	0.00
2b	C$_2$H$_5$	H	1.10 ± 0.03	0.54	−0.10
2c	n-C$_3$H$_7$	H	1.00 ± 0.03	0.49	−0.12
2d	Ph	H	5.86 ± 0.39	2.84	+0.60
2e	CH$_2$Ph	H	2.04 ± 0.03	0.99	+0.22
2f	CH$_3$	OCH$_3$	0.93 ± 0.04	0.45	
7 (Se)	CH$_3$	H	1.17 ± 0.01	0.57	

^{a} Calculated from the Arrhenius plot (see Supporting Information).
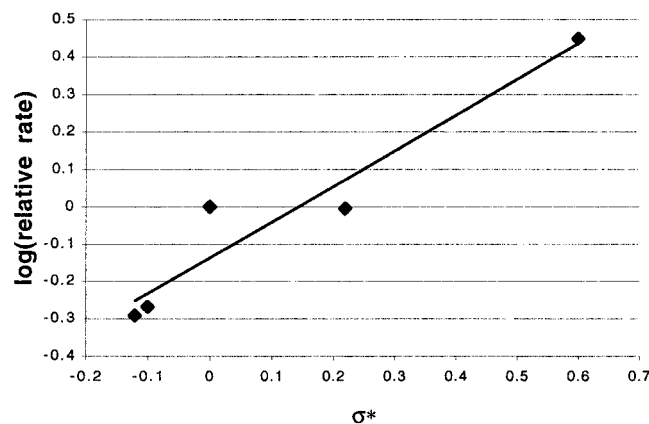
Figure 1. Rate of decomposition of nitrosimines **2** in methanol at 62.5° versus Taft σ^* steric parameter. $R^2 = 0.92$.

The primary focus of this experimental work was the kinetics of the decomposition of nitrosiminobenzothiazolines **2a**−**f**. The kinetics were measured by monitoring the disappearance of the nitrosimine absorptions at 340−360 nm over time. The raw kinetic data are presented and shown graphically in the Supporting Information. Control experiments demonstrated that 3-methyl-2-nitrosiminobenzothiazoline (**2a**) in methanol follows Beer's law over the range of concentrations $(2.97-9.35) \times 10^{-5}$ M and this method gave reproducible experimental rates. (See Figures S1 and S2, Supporting Information.) The decomposition of the substituted nitrosiminobenzenothiazolines **2a**−**f** and the selenium analogue **7** followed good first-order kinetics. The measured rate constants are reported in Table 1.

The rate of deazetization is only slightly affected by changes in the 3- and 6-substituents. The largest change is for phenyl substitution (**2d**) which increases the rate by a factor of 2.84 compared with **2a**, while addition of a 6-methoxy substituent (**2f**) reduces the rate by a factor of 0.45. This admittedly limited range of substituents showed a good correlation with the Taft σ^* (steric) parameter,[16] as shown in Figure 1. Replacement of sulfur in **2a** by selenium in **7** likewise makes only a modest effect, reducing the rate by a factor of 0.57.

Changing the solvent has only a modest effect on the rate of decomposition of **2a** (Table 2). The rate is fastest in cyclohexane and slowest in acetonitrile. The temperature dependence of the rate of decomposition of **2a** was determined in both methanol and cyclohexane. The derived activation energies (E_a), enthalpies ($\Delta H^\ddagger$), and entropies ($\Delta S^\ddagger$) are presented in Table 3.

The decompositions of **2a**−**f** and **7** follow first-order kinetics. This would be consistent either with the proposed mechanism in eq 2 or with a radical fragmentation mechanism (eq 3). In a radical mechanism, the substituents would be expected to have a larger influence on the rate, particularly comparing the phenyl

(16) Lowry, T. H.; Richardson, K. S. *Mechanism and Theory in Organic Chemistry*, 3rd ed.; Harper & Row: New York, 1987.

Table 2. Rates of Decomposition of 3-Methyl-2-nitrosiminobenzothiazoline (**2a**) in Various Solvents at 62.3°

solvent	$k_1 \times 10^5$, sec^{-1}	relative rate	Z, kcal/mol^b
acetonitrile	0.94 ± 0.01	0.46	71.3
methanol	2.06^a	1.00	83.6
1,4-dioxane	3.35 ± 0.05	1.61	66^c
cyclohexane	19.2 ± 0.6	9.32	54

^{a} Calculated from the Arrhenius plot (see Supporting Information). ^{b} Z value, as a measure of solvent polarity, ref 17. ^{c} Estimated from the data for acetone.

Table 3. Activation Energies (E_a), Enthalpies ($\Delta H^\ddagger$) and Entropies ($\Delta S^\ddagger$) for the Decomposition of 3-Methyl-2-nitrosiminobenzothiazoline (**2a**) in Cyclohexane and Methanol

solvent	E_a, kcal/mol	$\Delta H^\ddagger$, kcal/mol	$\Delta S^\ddagger$, eu^a
methanol	23.1 ± 0.71	22.5 ± 0.7	−12.9 ± 2.1
cyclohexane	26.0 ± 0.50	25.3 ± 0.5	1.3 ± 1.5

^{a} Calculated at 60°.

substitutent in **2d** and the substitution of Se for S in **7**. However, the observed substituent effects are very small. Furthermore, the products are not consistent with those expected from a radical pathway, such as appears to be operative in the photochemical deazetization of **2**.[12] Finally, the activation entropies, $\Delta S^\ddagger$ of 1.3 eu in cyclohexane and of −12.9 eu in methanol, are inconsistent with the large and positive activation entropy anticipated for a fragmentation reaction. Thus, all of these results are consistent with the mechanism presented in eq 2.

Changing from a nonpolar to a polar solvent makes only small changes in the rate. Qualitatively, the reaction is faster in cyclohexane, the least polar solvent. This indicates that the transition state is less polar than the reactants **2a**. This is reasonable, given that polar, delocalized resonance structures can be drawn for nitrosimines. However, the reaction is only 21 times slower in acetonitrile at 62.3°, indicating that there are not significant changes in polarity between **2a** and the transition state. Quantitatively, the rate for decomposition of **2a** does not correlate well with the Z value as a measure of the solvent polarity (Table 2).[17] Methanol is the most polar of the four solvents studied, but the rate is slowest in acetonitrile and fastest in cyclohexane. It could be that there is some hydrogen bonding between the nitrosimine and methanol that is enhanced in the transition state, and this increases the rate. This would be consistent with the more negative value of $\Delta S^\ddagger$ (−12.9 eu) measured for the deazetization in methanol as compared to that in cyclohexane (1.3 eu)

As originally proposed, deazetization of **2** might proceed via the intermediate **3** (eq 2). This is a unimolecular reaction, in agreement with the observed first-order kinetics. The intermediates **3** would be expected to be less polar than the nitrosimines **2**, consistent with the slower rates measured in more polar solvents. The change in hybridization from sp^2 to sp^3 would increase steric crowding between R$_1$ and R$_2$ in acyclic nitrosimines **1** and would disrupt the heteroaromaticity of **2**. Thus, this proposed mechanism is also consistent with the solvent effects and the stability trends.

Theoretical Studies

An ab initio study of the two-step pathway was undertaken with the expectation that it would provide additional insight

(17) Kosower, E. M. *J. Am. Chem. Soc.* **1958**, *80*, 3235.

Table 4. Relative Energies (kcal/mol) for the Reactions of **9a**, **9b**, and **13**, Optimized at the MP2/6-31G* level

structure	RHF/6-31G*[a]	MP2[b]	MP2[b]ΔG	MP3[b]	MP4(SDQ)[b]	MP4[b]+ZPE[c]
			R = H			
9a	0.00	0.00	0.00	0.00	0.00	0.00
9a(out)	−2.56	2.62	1.67	−0.57	0.35	0.23
9a′	0.94	3.17	2.62	2.25	2.66	2.67
9a′(out)	−0.98	4.52	3.62	1.30	2.43	2.34
ΔE(rot)[d]	17.36	17.64	17.01	18.06	17.29	16.61
ΔE(rot)-out[e]	18.59	17.39	16.32	18.33	17.68	16.74
9aTS	27.99	23.95	23.13	24.00	22.28	21.51
10a	18.74	19.78	18.71	14.35	15.97	15.00
10aTS	36.65	28.57	26.29	28.78	27.29	25.22
11a + N₂	−107.76	−89.95	−102.96	−90.89	−92.76	−95.53
			R = CH₃			
9b	0.00	0.00	0.00	0.00	0.00	0.00[f]
9b′	10.80	11.55		11.08	10.96	9.91[f]
9bTS	27.42	22.59		22.70	21.00	20.32[f]
10b	20.51	20.94		15.96	17.25	17.18[f]
10bTS	36.37	28.28		27.93	26.60	24.76[f]
11b + N₂	−105.73	−87.43		−92.61	−92.33	−94.72[f]
			Homolytic Fragmentation[g]			
12 + NO		55.7	45.8	38.5	38.7	40.0
13 + NO		47.8	35.5	36.6	33.3	33.7
			Oxetene Ring Opening			
15	33.50	27.31	28.88	26.71	28.60	29.46
15TS	68.64	55.61	55.77	60.47	58.85	58.39
16	0.00	0.00	0.00	0.00	0.00	0.00

[a] Optimized at the RHF/6-31G* level. [b] Calculated using the 6-31G* basis set and the frozen core approximation. [c] Zero-point vibrational energy correction from MP2/6-31G* frequencies and scaled by 0.9646. [d] **9a-rot-ts**, barrier height between **9a** and **9a′**. [e] **9a-rot-ts-out**, barrier height between **9a(out)** and **9a(out)′**. [f] Zero-point vibrational energy correction from RHF/6-31G* frequencies and scaled by 0.9135. [g] Energies relative to **9a**.

into the nature of the reaction. Nitrosimines **9a** and **9b** (eq 5) were chosen as simplified models of the experimental system. These retain the essential electronic features, namely the nitrosimine functionality and the thiazole ring, without the computational complexity of the fused benzene ring and additional nitrogen substituents. The experimental activation barrier for the deazetization of 3-methyl-2-nitrosiminobenzothiazoline (**2a**) is 25.3 kcal/mol in cyclohexane and 22.5 in methanol. Since there is only a small solvent effect on the rate of the decomposition, the calculated gas-phase activation barriers for the reactions of **9** might be expected to be comparable to the experimental values, particularly in cyclohexane. The steric and electronic effects of an alkyl substituent on the ring nitrogen (N₃) were probed by the methyl derivative **9b**. The loss of NO and the ring opening of the resulting radical were modeled by **12** and **13**, respectively.

(5)

R=H   **9a**   **10a**   **11a**
R=CH₃ **9b**   **10b**   **11b**

12 + NO ⇌ **13**
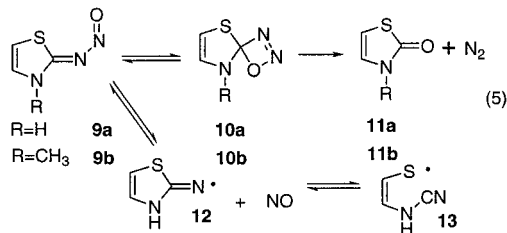
Computational Methods

The geometries and energies of the ground-state conformations as well as transition states along the reaction pathway were calculated with ab initio molecular orbital theory using Gaussian 94.[18] Geometries were optimized first at the RHF/6-31G* level and then reoptimized at the MP2(FC)/6-31G* level. Frequency calculations verified the identity of each stationary point as a minimum or transition state; these were done at both levels for the hydrogen substituent and at the RHF/6-31G* level for the methyl substituent. Single-point energies of each structure were

Table 5. CHELPG Charges for the Decomposition of Nitrosimines **9a** and **9b** Using RHF/6-31G* Wave Functions at the MP2/6-31G* Optimized Geometries

	9a	9a′	9a-rot-ts	9aTS	10a	10aTS	11a
S₁	0.095	−0.060	0.101	0.045	−0.088	−0.061	−0.057
C₂	0.847	0.652	0.732	0.953	1.029	0.907	0.590
N₃	−0.554	−0.136	−0.492	−0.624	−0.703	−0.521	0.036
C₄	−0.033	−0.315	0.005	−0.035	0.017	−0.067	−0.102
C₅	−0.398	−0.133	−0.298	−0.339	−0.321	−0.290	−0.250
N₆	−0.633	−0.543	−0.681	−0.649	−0.466	−0.328	
N₇	0.158	0.135	0.166	0.202	0.143	0.145	
O₈	−0.357	−0.391	−0.391	−0.516	−0.457	−0.610	−0.564

	9b	9b′	9bTS	10b	10bTS	11b
S₁	0.053	0.018	0.044	−0.049	−0.027	−0.064
C₂	0.732	0.608	0.760	0.813	0.726	0.476
N₃	−0.200	−0.064	−0.228	−0.299	−0.184	0.041
C₄	−0.119	−0.156	−0.068	−0.031	−0.092	−0.226
C₅	−0.338	−0.266	−0.343	−0.364	−0.336	−0.243
N₆	−0.509	−0.562	−0.553	−0.441	−0.302	
N₇	0.086	0.108	0.165	0.130	0.125	
O₈	−0.328	−0.338	−0.479	−0.401	−0.544	−0.532
C₉	0.040	−0.011	0.081	0.026	−0.004	−0.089

calculated at the MP4(FC,SDQ)/6-31G* level with the MP2(FC)/6-31G* optimized geometries. The zero-point vibrational energy (ZPE) corrections were obtained by scaling the RHF/6-31G* ZPE by 0.9135, or the MP2/6-31G*(FC) ZPE by 0.9646 as recommended by Pople et al.[19] Unless otherwise indicated, all energies discussed in the text are MP4(SDQ,FC)/

(18) Frisch, M. J.; Trucks, G. W.; Schlegel, H. B.; Gill, P. M. W.; Johnson, B. G.; Robb, M. A.; Cheeseman, J. R.; Keith, T.; Petersson, G. A.; Montgomery, J. A.; Raghavachari, K.; Al-Laham, M. A.; Zakrzewski, V. G.; Ortiz, J. V.; Foresman, J. B.; Peng, C. Y.; Ayala, P. Y.; Chen, W.; Wong, M. W.; Andres, J. L.; Replogle, E. S.; Gomperts, R.; Martin, R. L.; Fox, D. J.; Binkley, J. S.; Defrees, D. J.; Baker, J.; Stewart, J. P.; Head-Gordon, M.; Gonzalez, C.; Pople, J. A. *Gaussian 94*, revision B.3; Gaussian, Inc.: Pittsburgh, PA, 1995.
(19) Pople, J. A.; Scott, A. P.; Wong, M. W.; Radom, L. *Isr. J. Chem.* **1993**, *33*, 345−350.
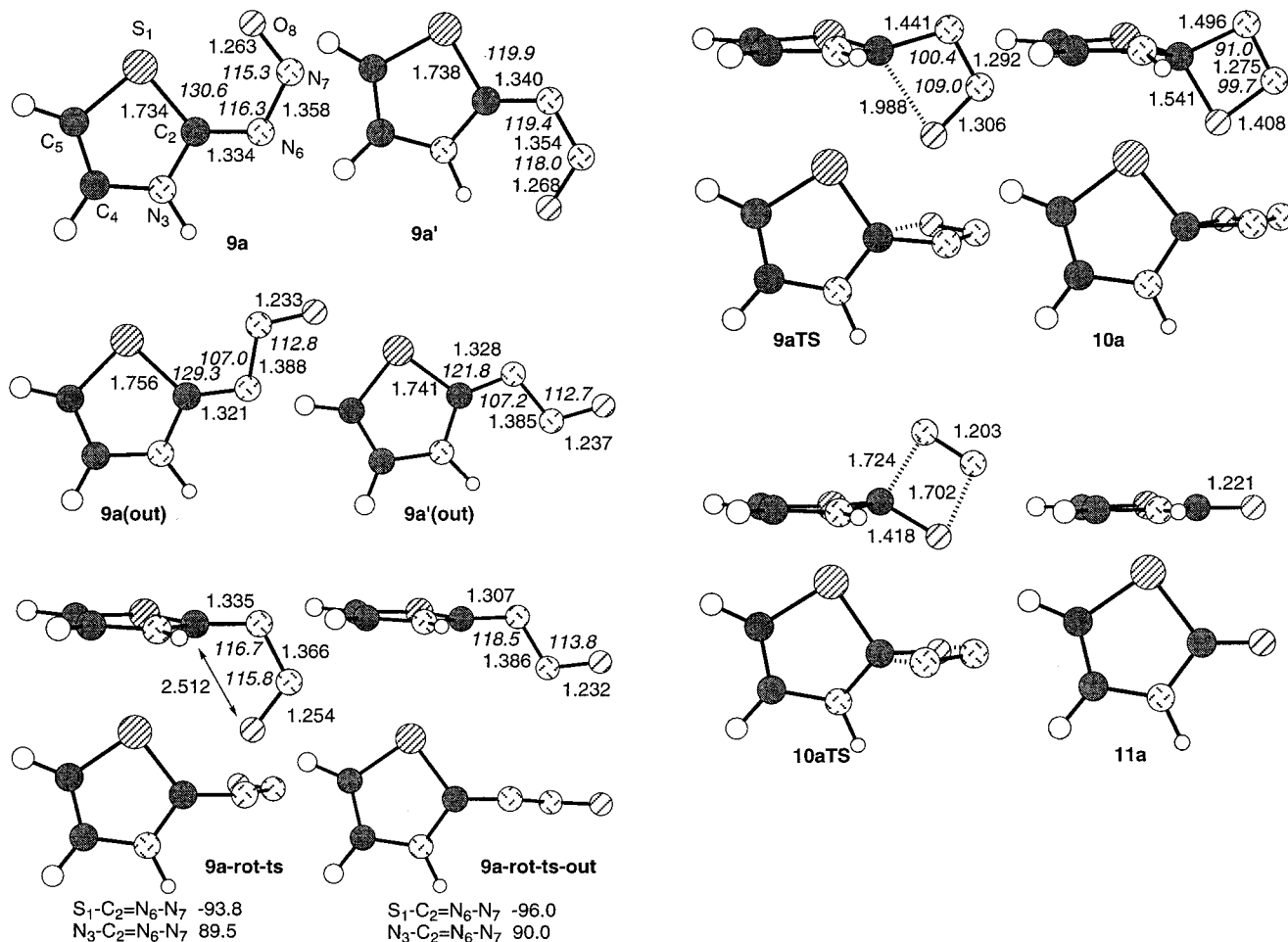
Figure 2. MP2/6-31G* optimized geometries of conformations of **9a**, rotational transition states **9a-rot-ts** and **9a-rot-ts-out**, transition states **9aTS** and **10aTS**, and structures **10a** and **11a**. Distances are in Å, *angles in degrees*. The atom numbering and shadings are as shown for **9a**.

6-31G*//MP2(FC)/6-31G* level with the ZPE correction. Absolute energies are reported in the Supporting Information, and relative energies are reported in Table 4. Geometries optimized at the MP2(FC)/6-31G* level are shown in Figures 2, 6, and S9. CHELPG charges are given in Table 5.[20] Atom numbering follows **9a** in Figure 2 or **15** in Figure 5.

The four possible conformations of **9a** were calculated as shown in Figure 2. The $C_2=N_6-N_7=O_8$ moiety is, in most cases, planar and thus can be either *s*-cis or *s*-trans.[21] The NO can be either syn or anti to the sulfur; the anti conformation (to the sulfur) is designated **9′**, while *s*-trans is designated as **out**. The geometries of the conformations of **9a** were calculated and are shown in Figure 2. It is clear from inspection of **9a′** that there is some steric crowding and that there is not room to accommodate replacement of the N_3H with an N_3-CH_3 group. The **9b′** conformation is distorted from planarity because of steric crowding between the nitrosimine and the *N*-methyl groups (Figure S9). The bond angles of the **in** conformations are more open than those in the **out** conformations, again reflecting crowding. The **out** conformations show slightly more pronounced alternation in the $C_2=N_6$, N_6-N_7, and $N_7=O_8$ bond lengths; there is no obvious reason for this subtle trend. Although there is some variation, **9a** is calculated to be the most stable conformation at most levels of theory, while **9a(out)** is

calculated to be relatively close in energy. The anti conformations (**9a′** and **9a′(out)**) are consistently higher in energy, which is also consistent with steric crowding in these conformations.
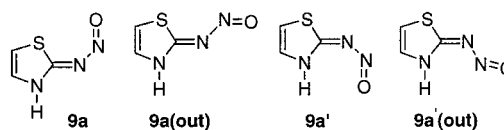
The homolytic bond strength of the N−NO bond was calculated to be 40.0 kcal/mol, (Table 4) on the basis of the formation of NO and **12** from **9a** (eq 5). For comparison, the experimental bond strengths for *N*-nitrosoureas are in the range of 23.1−33.1 kcal/mol.[2b] Although accurate calculation of radicals is difficult,[22] these results suggest that homolysis is not a facile process. The ring-opened radical **13** is calculated to be 6.3 kcal/mol more stable than **12**, consistent with the observation of ring-opened products in the photochemistry of **2** (eq 3).[12]

We located transition states for the isomerization of **9a** to **9a′** and of **9a(out)** to **9a(out)′**. These both correspond to rotations around the $C_2=N_6$ bond. The barriers for these rotations are comparable, and both are fairly low, 16.61 and 16.69 kcal/mol, respectively. The transition states are very close to symmetrical; the $N_3-C_2=N_6-N_7$ and $S_1-C_2=N_6-N_7$ dihedral angles in **9a-rot-ts** are 89.0° and −93.8°, respectively, and 90.0° and −96.0° in **9a-rot-ts-out**, respectively. Rotation does

(20) Breneman, C. M.; Wiberg, K. B. *J. Comput. Chem.* **1990**, *11*, 361−373.

(21) Nitrosamines also are planar, with hindered rotation.[6c] In contrast, nitrosiminoformaldehyde ($H_2C=N-N=O$) is nonplanar with a C−N−N−O dihedral angle of 71.5° at the MP2/6-31G* level.

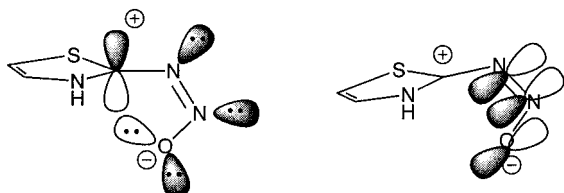(22) Hrovat, D., A.; Morokuma, K.; Borden, T., Weston. *J. Am. Chem. Soc.* **1994**, *116*, 1072−1076.

Figure 3. Selected basis orbitals of **9a-rot-ts**.

not dramatically change the C_2=N_6 bond length, although it is *shortened* from 1.321 or 1.328 Å in **9a(out)** or **9a′(out)** to 1.307 Å in **9a-rot-ts-out**. Similarly, the bond length of 1.335 Å in **9a-rot-ts** compares with bond lengths of 1.334 and 1.340 Å in **9a** and **9a′**, respectively. This reflects, at least in part, a change toward sp hybridization; as the bond rotates, the C_2=N_6–N_7 angles open from 116.3° and 107.0° in **9a** and **9a(out)**, respectively, to 116.7° and 118.5° in **9a-rot-ts** and **9a-rot-ts-out**, respectively. Clearly the π-bond is not completely broken at the transition state. This is not surprising; partial π-bonding is possible between the N_6-lone pair and the C_2-p orbital as shown in Figure 3. There is also a relatively small charge redistribution at the transition states; only −0.07 esu are transferred from the N_6–N_7=O_8 moiety on going from **9a** to **9a-rot-ts** (Table 5). There does not appear to be substantial bonding between the C_2 and O_8 in **9a-rot-ts**; the C_2–O_8 bond distance is 2.512 Å, and the N_6–N_7=O_8 bond angle of 115.8° is actually wider than in **9a-rot-ts-out**, where it is 113.8°.

The spirobicyclic intermediate **10a** was located. There is nothing particularly notable about the geometry of this structure; the bond lengths and angles are as would be expected for this strained intermediate. It is less polar than **9a**; N_6–N_7–O_8 moiety bears a −0.780 esu charge in **10a** as compared to 0.832 esu in **9a** (Table 5). This decrease in polarity is consistent with the observed solvent effects for **2a**, for which deazetization is faster in less polar solvents (Table 2).

A transition structure (**9aTS**) for the electrocyclization of **9a** to generate **10a** (eq 5) was also located. The geometry of **9aTS** is remarkably similar to the rotational transition state **9a-rot-ts** described above. The C_2–N_6 bond remains close to the plane of the ring. As would be expected, the C_2–N_6 and N_7–O_8 bonds lengthen (by 0.106 and 0.052 Å, respectively), while the N_6–N_7 distance shortens by 0.74 Å as compared to **9a-rot-ts**. The major difference between the two structures is the C_2–O_2 distance, which is reduced from 2.512 Å in **9a-rot-ts** to 1.988 Å in **9aTS**. One might question whether two distinct transition states with such similar geometries can exist for such different reactions, rotation and cyclization. The frequency calculations confirm that both are true transition states. The potential energy surface is represented in Figure 4. The transition structure **9aTS** connects two stationary points, **10a** and **9a-rot-ts**; it just happens that the latter of these stationary points is itself a transition state in an orthogonal direction, namely rotation about the C_2=N_6 bond.[23] This unusual potential energy surface has an analogy in the potential energy surface of cyclooctatetraene (**14**), for which the delocalized D_{8h} structure (**14TS′**) is a transition state connecting the localized D_{4h} structures (**14TS**), which are themselves transition states for the ring-inversion process (eq 6).[24] The symmetry constraints on this system in particular and of degenerate reactions in general have recently been discussed by Schaad and Hu.[25] Transition structure **9aTS**, although not degenerate, is consistent with their analysis. We note that the
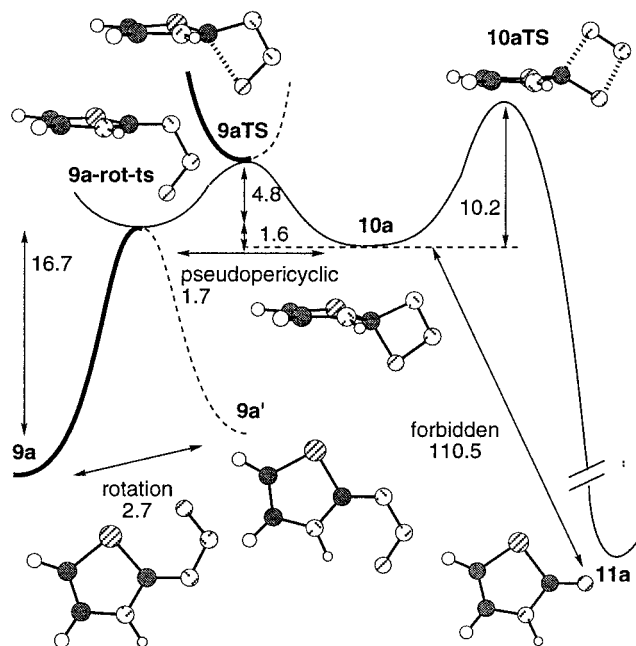

Figure 4. Potential energy surface for the deazetization of **9a**. Geometries are optimized at the MP2/6-31G* level. Relative energies are at the MP4(SDQ, FC)/6-31G* + ZPE level. The in-plane reaction coordinate corresponds to in-plane motions leading to cyclization and deazetization, while the out-of-plane coordinate corresponds to rotation around the C_2–N_6 bond. See text for a discussion of the relationship between **9a-rot-ts** and **9aTS**.

existence of two transition states does not require that the actual reaction trajectory of a given molecule pass through **9a-rot-ts**, but it will pass close to **9aTS**.
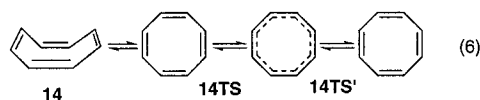
The overall barrier to formation of **10a** from **9a** is 21.5 kcal/mol. However, most of this barrier arises from the barrier to rotation from **9a** to **9a-rot-ts** (16.6 kcal/mol). The barrier for the ring closure from **9a-rot-ts** to **10a** is 4.9 kcal/mol and for the ring-opening from **10a** to **9a** is 6.5 kcal/mol. When viewed from this perspective, the calculated barriers for this electrocyclic reaction are remarkably low! This is because the transition state is pseudopericyclic.[26] The C_2–O_8 bond distance changes, but the C_2=N_6–N_7=O_8 system remains essentially planar and there are no changes in orbital overlap in the N_6–N_7=O_8 π-system. Without a loop of interacting orbitals, electron–electron repulsion can be minimized. This is indeed the case, since O_8 and C_2 are attracted to each other with calculated charges of −0.516 and 0.953 esu, respectively, in **9aTS**.

The ring-opening reaction of oxetene (**15**, eq 4) might be viewed as an analogous model system for the ring-opening of **10a** via **9aTS**. Although the reaction of oxetene to give acrolein (**16**) has previously been calculated at the CASSCF/6-31G*// RHF/6-31G* level[11] and the geometry of acrolein has been reported at the MP2/6-31G* level,[27] the geometries of **15** and **15TS** were reoptimized at the MP2/6-31G* level for the comparison with the reaction of **10a** to **9a** and are shown in Figure 5. The activation barrier calculated here for the ring-

(23) Rotation at the geometry of **9aTS** raises the energy of the system because it breaks the partially formed C_2–O_8 bond.

(24) Wenthold, P. G.; Hrovat, D. A.; Borden, W. T.; Lineberger, W. C. *Science* **1996**, *272*, 1456−1459.

(25) Schaad, L. J.; Hu, J. *J. Am. Chem. Soc.* **1998**, *120*, 1571−1580.

(26) (a) Birney, D. M.; Wagenseller, P. E. *J. Am. Chem. Soc.* **1994**, *116*, 6262−6270. (b) Birney, D. M.; Xu, X.; Ham, S. *Angew. Chem., Int. Ed.* **1999**, *38*, 189−193.
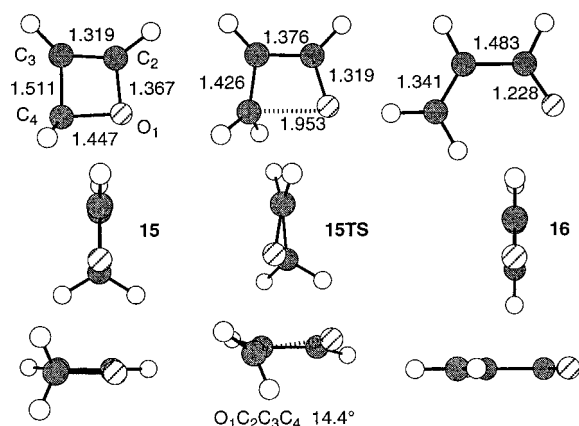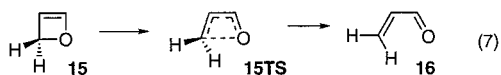
Figure 5. MP2/6-31G* optimized geometries for **15**, **15TS**, and **16**. See Figure 2 for key; atom numbering is as shown for **15**.

opening reaction of oxetene via **15TS** is 28.9 kcal/mol (MP4-(SDQ)/6-31G*//MP2/6-31G* + ZPE). This compares more favorably with the experimental activation enthalpy of 24.1 ± 1.5 kcal/mol,[28] than does the CASSCF/6-31G*//RHF/6-31G* barrier of 32.2 kcal/mol. The barrier calculated here (**15TS**) is 22.4 kcal/mol higher than for the comparable reaction of **10a**. Significantly, the exothermicity for the ring-opening of oxetene is calculated to be 29.5 kcal/mol, whereas for the reaction of **10a** to **9a-rot-ts** it is 1.7 kcal/mol. The remarkably lower barrier for the ring-opening of **10a**, especially in light of the modest calculated exothermicity, is consistent with the low barriers found for other pseudopericyclic reactions when the geometry and electrostatic interactions are favorable.[29] Comparing the geometries of both transition structures optimized at the MP2/6-31G* level, **9aTS** is essentially planar with a $C_2N_6N_7O_8$ dihedral angle of 2.3°. The corresponding dihedral angle in the transition state of oxetene ring-opening (**15TS**) is 14.4°. This reflects the need for rotation of the CH_2 moiety to accommodate developing π-overlap in the transition state, as is typical in pericyclic reactions.[10,30] In principle, oxetene ring-opening could proceed via an analogous two-stage process, with a planar, pseudopericyclic transition state connecting to a transition state for rotation around the $C_4—C_3$ bond. The difference between the two systems is that the barriers for bond breaking in **15** and for rotation around the $C_4=C_3$ bond in acrolein (**16**) are much higher than for **10a** and **9a**; thus, there is an energetic benefit to twisting in the ring-opening of oxetene, which allows for partial p-overlap in the transition state **15TS**. From this perspective then, the ring closure of **9a** to **10a** may be considered to have decoupled the two fundamental processes, rotation and bond formation, which are required for the overall pericyclic process.

$$\text{(7)}$$

Finally, transition structure **10aTS** for the [2 + 2]-cycloreversion of **10a** to form **11a** and N_2 was located (eq 5). The activation barrier for this elementary reaction step is calculated

to be 10.2 kcal/mol. The Hammond postulate[31] would predict that this should have a low barrier because it is very exothermic. Indeed, the exothermicity of the retro [2 + 2] reaction to form **11a** is calculated to be 95.5 kcal/mol, and the exoergonicity is calculated to be 103.0 kcal/mol (unscaled ΔG at the MP2/6-31G* level). This reflects the relief of ring strain in the transition state, as well as the greater strengths of the C=O π-bond and of the second N=N π-bond. There is also a significant, favorable entropic contribution to the exoergonicity of the reaction simply due to the formation of two products. It is noteworthy that the barrier of 10.2 kcal/mol for the formation of **11a** and N_2 from **10a** is higher than the 6.5 kcal/mol for the ring-opening reaction of **10a** to give **9a** via **9aTS**. Indeed, if **9aTS** is considered to be the transition state connecting **10a** to **9a-rot-ts**, then this is indeed endothermic by 1.6 kcal/mol, yet has a lower barrier. This is not surprising, because the [2 + 2]-cycloreversion is orbital-symmetry-forbidden, while the electrocyclization is allowed and is pseudopericyclic.[29a] Thus, the overall gas-phase barrier for this deazetization reaction (**9a** to **10aTS**) is calculated to be 25.2 kcal/mol. This compares very favorably with the experimental barrier of 25.3 kcal/mol for the deazetization of 3-methyl-2-nitrosiminobenzothiazoline (**2a**) in cyclohexane. Furthermore, **10aTS** is calculated to be less polar than **9a**; the $N_6—N_7—O_8$ moiety in **10aTS** is calculated to have a −0.793 esu charge as compared to −0.832 esu in **9a** (from Table 5). This is consistent with the observed solvent effects for the deazetization of **2a** (Table 2).

The overall entropy of the deazetization reaction (**9a** to **10aTS**) was calculated to be + 0.9 eu This ignores statistical contributions from the multiple conformations of **9**, as well as the existence of enantiomeric transition states **10aTS**. This small, positive entropy of activation is consistent with the experimental value of +1.3 eu measured for **2a** in cyclohexane.

Similar results were obtained with methyl substitution on the ring nitrogen, **9b**, **9b′**, **9bTS**, **10b**, **10bTS**, and **11b**. These structures are shown in Figure S9 in the Supporting Information. With the exception of **9b′**, there are not significant differences in geometries between the hydrogen and methyl series. As discussed above, steric hindrance in **9b′** between the $N_6—N_7=O_8$ and the methyl group force $N_6—N_7=O_8$ to twist out of plane (the $N_3—C_2=N_6—N_7$ dihedral angle is 48.3 °). The methyl group does not make a significant difference to the calculated barrier of 24.8 kcal/mol for **10bTS** as compared to 25.2 kcal/mol for **10aTS**. This is consistent with the experimental results which do not show significant changes in rate as the ring nitrogen (N_3) substituent is varied.

Conclusions

Ab initio calculations suggest that the deazetization of nitrosiminothiazolines can be understood as a three-stage reaction. Beginning from one of the inward conformations, for example, **9a** or **9a′**, the first stage involves rotation of $N_6—N_7=O_8$ out of the plane to a rotational transition state, **9a-rot-ts**. This transition state positions these atoms so that they can cyclize in the second stage, without passing through a separate intermediate, via a low-barrier, pseudopericyclic transition state (**9aTS**) to the spirobicyclic intermediate **10a**. This two-stage process is qualitatively different from the single-stage process for the pericyclic ring-opening of oxetene (**15**). However, the pericyclic process can be understood as a compromise between the two fundamental steps, rotation and pseudopericyclic ring closure. Next, in the rate-determining step, this undergoes an orbital-symmetry-forbidden, but extremely exothermic, deazeti-

(27) Wiberg, K. B.; Rosenberg, R. E.; Rablen, P. R. *J. Am. Chem. Soc.* **1991**, *113*, 2890−2898.

(28) Martino, P. C.; Shevlin, P. B. *J. Am. Chem. Soc.* **1980**, *102*, 5429−5430.

(29) (a) Birney, D. M.; Ham, S.; Unruh, G. R. *J. Am. Chem. Soc.* **1997**, *119*, 4509−4517. (b) Birney, D. M. *J. Am. Chem. Soc.* **2000**, *122*, 10917−10925.

(30) Spellmeyer, D. C.; Houk, K. N. *J. Am. Chem. Soc.* **1988**, *110*, 3412−3416.

(31) Hammond, G. S. J. *J. Am. Chem. Soc.* **1955**, *77*, 334−338.

zation via **10aTS** to form the products **11a** and N_2. The overall calculated gas-phase barrier of 25.2 kcal/mol compares favorably with the experimental barrier of 25.3 kcal/mol for the deazetization of 3-methyl-2-nitrosiminobenzothiazoline (**2a**) in cyclohexane. This proposed mechanism is also consistent with the observed modest solvent and substitutent effects on the rate. Homolytic fragmentation of **9a** to **12** and NO is calculated to be 40.0 kcal/mol endothermic; the larger barrier explains why homolysis is not generally observed under thermal conditions.

Experimental Procedures

The substituted iminobenzothiazolines **6a** (mp 124−125 °C), **6f** (mp 94−94.5 °C), and 3-methyl-2-iminobenzoselenazoline (mp 101−105 °C) were obtained from the laboratories of Professor S. Hünig of the University of Würtsburg. ^{1}H NMR spectra were recorded at 60 MHz with a Varian A-60 spectrometer, in $CDCl_3$ as solvent. UV spectra were recorded using a Cary 15 UV/vis spectrometer.

Preparation of 3-Methyl-2-nitrosiminobenzothiazoline (2a). Into a pear-shaped flask, fitted with a pressure-equilibrating addition funnel and magnetic stirrer, were placed 1.00 g (6.1 mmol) of 3-methyl-2-iminobenzothiazoline (**6a**, obtained from the laboratories of S. Hünig, mp 124−125 °C) and 7.4 mL of glacial acetic acid. The resulting solution was cooled with an ice bath. A sodium nitrite solution, 3.0 mL (8.7 mmol of sodium nitrite), was added dropwise. The color of the solution changed from colorless to yellow-gold to orange, and an orange precipitate of the nitrosimine **2a** formed. After filtering the solution, the nitrosimine was washed several times with water and dried in vacuo over silica gel. The chemically pure nitrosimine (0.98 g, 75.6%) mp 152−153 °C (reported 152 °C).[9a] IR 1540, 1390; ^{1}H NMR 3.90 (s, 3H), 7.27−7.88 (m, 4H).

Preparation of nitrosimines **2b**−**f** and **7** and of intermediates **5** and **6** are described in the Supporting Information.

Kinetic Studies of the Thermal Decomposition of 3- and 3,6-Substituted 2-Nitrosiminobenzothiazolines. A solution of the desired heterocyclic nitrosimine−solvent combination was prepared in a volumetric flask by dissolving the nitrosimine in the requisite solvent. Dissolution in cyclohexane required stirring with a magnetic stirring bar for several hours at room temperature. During this period, the volumetric flasks were wrapped in aluminum foil.

Portions of the solutions were sealed in nitrogen-flushed glass ampules, and the ampules were wrapped in aluminum foil. The ampules were immersed in a constant-temperature bath. After the desired reaction time, ampules were removed and cooled in an ice−water bath to quench the reaction.

The ultraviolet spectrum of the solution was then examined for absorption of the nitrosimine in the region of 345 nm. Summaries of

kinetic data and the absorption maxima for various nitrosimines in methanol and for 3-methyl-2-nitrosiminobenzothiazoline (**2a**) in various solvents are given in Tables S1, S2, and S3 in the Supporting Information. Linear regression least-squares analysis of ln absorption versus time gave the first-order rate constants. The standard deviations of the slopes gave the estimated errors in the first-order rate constants.

Calculation of Activation Parameters. Since first-order rate constants for the thermal decomposition of **2a** were determined at several different reaction temperatures in methanol and cyclohexane, activation parameters could be evaluated. Linear regression least-squares analysis of ln k versus $1/T$ gave the Arrhenius activation energy. The error in the activation energy was taken to be the standard deviation of the slope.

Product Study of the Thermal Decomposition of 3-Methyl-2-nitrosiminobenzothiazoline (2a) in Methanol. By using the procedure outlined above for the kinetic studies, solutions of 3-methyl-2-nitrosiminobenzothiazoline (**2a**) in methanol were prepared. The resulting solutions were sealed in ampules and placed in a 62.3° constant-temperature bath for 58 h. This period corresponded to 5.1 half-lives of the kinetic reaction.

The ultraviolet spectra of the solutions were examined for absorption at $\lambda_{max} = 288$ nm which is due to 3-methyl-2-benzothiazolinone. By comparison of the absorbance with that of known concentrations of 3-methyl-benzothiazolinone (**4a**) in methanol (Figure S1 and Table S4, Supporting Information) at $\lambda_{max} = 288$ nm, the yield of 3-methyl-2-benzothiazolinone (**4a**) was calculated (Table S5, Supporting Information). Thus, a $101.8 \pm 0.5\%$ yield of 3-methyl-2-benzothiazolinone was obtained. The slightly higher than 100% yield of 3-methyl-2-benzothiazolinone (**4a**) is probably due to errors introduced by the low absorbance of the product when compared to that of the reactant.

Supporting Information Available: Experimental details for the preparation and characterization of nitrosimines **2b**−**f** and **7** and of intermediates **5** and **6**, kinetic data and molar absorptivities and Beer's law, log absorbance vs time and Arrhenius plots, MP2/6-31G* optimized Cartesian coordinates, vibrational frequencies, and a table of absolute energies for all calculated stationary points are provided (PDF). This material is available free of charge via the Internet at http://pubs.acs.org.